K. Lindfors, L. Lechner, and M. Kaivola. 2009. Dependence of resonant light transmission properties of a subwavelength slit on structural parameters. Optics Express, volume 17, number 13, pages 11026-11038.

Dependence of resonant light transmission properties of a subwavelength slit on structural parameters

K. Lindfors,[1*] **L. Lechner,**[2] **and M. Kaivola**[1]

[1] *Helsinki University of Technology (TKK), Department of Applied Physics and Center for New Materials, Espoo, FI-02150, Finland*

[2] *Helsinki University of Technology (TKK), Low Temperature Laboratory, Espoo, FI-02150, Finland*

klas.lindfors@tkk.fi

Abstract: We perform a systematic study of the resonant transmission of visible and near-infrared (NIR) light through a single subwavelength slit in a gold film when the parameters defining the structure are varied. We further examine the optical properties of a related nanostructure, a cross with subwavelength sized features. Focused ion beam (FIB) milling was used to fabricate nanoslits and crosses with linewidths ranging from 26 nm to 85 nm. The dimensions of the structure are found to affect strongly the transmittance spectrum. For example, as the slit becomes narrower the resonance is observed to both sharpen and shift significantly. Our observations are in good agreement with our earlier numerical calculations on the optical properties of nanoslits.

OCIS codes: (310.6628) Subwavelength structures, nanostructures; (050.1220) Apertures; (350.4238) Nanophotonics and photonic crystals

References and links

1. T.W. Ebbesen, H.J. Lezec H J, H.F. Ghaemi, T. Thio, and P.A. Wolff, "Extraordinary optical transmission through sub-wavelength hole arrays," Nature **391,** 667–669 (1998).
2. C. Genet and T.W. Ebbesen, "Light in tiny holes," Nature **445,** 39–46 (2007).
3. A. Degiron, H.J. Lezec, N. Yamamoto, and T.W. Ebbesen, "Optical transmission properties of a single subwavelength aperture in a real metal," Opt. Commun. **239,** 61–66 (2004).
4. F. Yang and J.R. Sambles, "Resonant Transmission of Microwaves through a Narrow Metallic Slit," Phys. Rev. Lett. **89,** 063901 (2002).
5. F.J. García-Vidal, H.J. Lezec, T.W. Ebbesen, and L. Martín-Moreno, "Multiple Paths to Enhance Optical Transmission through a Single Subwavelength Slit," Phys. Rev. Lett. **90,** 213901 (2003).
6. S. Astilean, Ph. Lalanne, and M. Palamaru, "Light transmission through metallic channels much smaller than the wavelength," Opt. Commun. **175,** 265–273 (2000).
7. Y. Takakura, "Optical Resonance in a Narrow Slit in a Thick Metallic Screen," Phys. Rev. Lett. **86,** 5601–5603 (2001).
8. J. Bravo-Abad, L. Martín-Moreno, and F.J. García-Vidal, "Transmission properties of a single metallic slit: From the subwavelength regime to the geometrical-optics limit," Phys. Rev. E **69,** 026601 (2004).
9. J.R. Suckling, A.P. Hibbins, M.J. Lockyear, T.W. Preist, J.R. Sambles, and C.R Lawrence, "Finite Conductance Governs the Resonance Transmission of Thin Metal Slits at Microwave Frequencies," Phys. Rev. Lett. **92,** 147401 (2004).
10. W.L. Barnes, A. Dereux, and T.W. Ebbesen, "Surface plasmon subwavelength optics," Nature **424,** 824–830 (2003).

#110533 - $15.00 USD Received 23 Apr 2009; revised 5 Jun 2009; accepted 7 Jun 2009; published 17 Jun 2009

11. A.V. Zayats, I.I. Smolyaninov, and A.A. Maradudin, "Nano-optics of surface plasmon polaritons," Phys. Rep. **408,** 131–314 (2005).
12. H.T. Miyazaki and Y. Kurokawa, "Squeezing Visible Light Waves into a 3-nm-Thick and 55-nm-Long Plasmon Cavity," Phys. Rev. Lett. **96,** 097401 (2006).
13. S. Collin, F. Pardo, R. Teissier, and J.-L. Pelouard, "Efficient light absorption in metal-semiconductor-metal nanostructures," Appl. Phys. Lett. **85,** 194–196 (2004).
14. W. Srituravanich, N. Fang, C. Sun, Q. Luo, and X. Zhang, "Plasmonic Nanolithography," Nano Lett. **4,** 1085–1088 (2004).
15. A.G. Brolo, E. Arctander, R. Gordon, B. Leathem, and K.L. Kavanagh, "Nanohole-Enhanced Raman Scattering," Nano Lett. **4,** 2015–2018 (2004).
16. C. Liu, V. Kamaev, and Z.V. Vardeny, "Efficiency enhancement of an organic light-emitting diode with a cathode forming two-dimensional periodic hole array," Appl. Phys. Lett. **86,** 143501 (2005).
17. J. Dintinger, I. Robel, P.V. Kamat, C. Genet, and T.W. Ebbesen, "Terahertz All-Optical Molecule-Plasmon Modulation," Adv. Mater. **18,** 1645–1648 (2005).
18. M. Leutenegger, M. Gösch, A. Perentes, P. Hoffmann, O.J.F. Martin, and T. Lasser, "Confining the sampling volume for Fluorescence Correlation Spectroscopy using a sub-wavelength sized aperture," Opt. Express **14,** 956–969 (2006).
19. K.A. Tetz, L. Pang, and Y. Fainman, "High-resolution surface plasmon resonance sensor based on linewidth-optimized nanohole array transmittance," Opt. Lett. **31,** 1528–1530 (2006).
20. K.-L. Lee, C.-W. Lee, W.-S. Wang, and P.-K. Wei, "Sensitive biosensor array using surface plasmon resonance on metallic nanoslits," J. Biomed. Opt. **12,** 044023 (2007).
21. J. Lindberg, K. Lindfors, T. Setälä, M. Kaivola, and A.T. Friberg, "Spectral analysis of resonant transmission of light through a single sub-wavelength slit," Opt. Express **12,** 623–630 (2004).
22. D.E. Aspnes, E. Kinsbron, and D.D. Bacon, "Optical properties of Au: Sample effects," Phys. Rev. B **21,** 3290–3299 (1980).
23. R. Gordon, "Light in a subwavelength slit in a metal: Propagation and reflection," Phys. Rev. B **73,** 153405 (2006).
24. I.P. Kaminow, W.L. Mammel, and H.P. Weber, "Metal-Clad Optical Waveguides: Analytical and Experimental Study," Appl. Opt. **13,** 396–405 (1974).
25. P.B. Johnson and R.W. Christy, "Optical Constants of Noble Metals," Phys. Rev. B **6,** 4370–4379 (1972).
26. J.A. Matteo, D.P. Fromm, Y. Yuen, P.J. Schuck, W.E. Moerner, and L. Hesselink, "Spectral analysis of strongly enhanced visible light transmission through single C-shaped nanoapertures," Appl. Phys. Lett. **85,** 648–650 (2004).
27. Ch. Wohlfarth and B. Wohlfarth, "Refractive Indices of Organic Liquids," in *Landolt-Börnstein Group III Condensed Matter vol 38B*, M.D. Lechner, ed. (Springer-Verlag, Berlin, 1996).

1. Introduction

The transmission of light through a thin metallic film perforated by an array of subwavelength apertures can, at resonant wavelengths, be significantly higher than the area fraction occupied by the holes would suggest [1]. After the initial discovery of enhanced optical transmission through nano-structured metallic thin films by Ebbesen *et al.* [1], a number of investigators have studied this phenomenon (see the recent review [2] and references therein). Such resonant transmission of light has more recently also been observed for individual holes [3] and slits [4, 5]. For arrays of holes, the enhanced transmission has been attributed to the excitation of surface plasmons that tunnel through the film and radiate on the other side of the metal [2]. A single subwavelength slit differs from individual holes or arrays of them as the slit can support propagating electromagnetic modes even when the width of the slit is made arbitrarily small [4, 5, 6, 7, 8, 9].

The optical properties of metallic nanostructures, such as perforated noble metal films, have attracted considerable interest both in fundamental studies of light-matter interaction and in developing photonic devices based on surface waves [10, 11]. For example, recently Miyazaki and Kurokawa demonstrated that light could be confined in $Au/SiO_2/Au$ waveguide-like nanostructures with SiO_2 cores of thickness down to 3 nm and that Fabry-Pérot-like resonances were exhibited in the longitudinal direction of the optical cavity [12]. In device development, perforated metal films have already been demonstrated in applications such as photodetection [13], lithography [14], Raman scattering [15], organic light-emitting diodes [16], switching [17],

#110533 - $15.00 USD Received 23 Apr 2009; revised 5 Jun 2009; accepted 7 Jun 2009; published 17 Jun 2009

fluorescence correlation spectroscopy [18], and biosensors [19, 20].

In this paper we study systematically the influence of the relevant structural parameters on the transmission of light through a single slit in a gold film, with a width much smaller than the wavelength of the incident light. Furthermore, we compare the light transmission properties of such a nanoslit and a cross composed of two orthogonal slits. The observed resonant transmission of light is explained using a simple model of waveguiding in the nanoslit. This work is a continuation to our earlier numerical study of nanoslit transmission reported in [21]. We find that the experimental results are in good agreement with the numerically calculated data.

The paper is organized as follows. In Sec. 2 we present the sample preparation procedure and the experimental methods used to characterize the nanostructures. The experimental results are analyzed in Sec. 3 and the main conclusions are summarized in Sec. 4.

2. Sample fabrication and experimental methods

The structures studied in this paper were fabricated by focused ion beam (FIB) milling of a gold film thermally evaporated on a microscope cover glass. The glass substrates were first sonicated in organic solvents, then rinsed in deionized water (DIW) followed by immersion in piranha solution. After cleaning in piranha, the substrates were thoroughly rinsed and stored in DIW until gold deposition. Gold (greater than 99.9 % purity) was thermally evaporated in a vacuum coating system from a resistive evaporation source. The film thickness was checked using a profilometer by recording the surface profile of several scratches in the gold film made close to the edge of the substrate. The thickness of the film was also estimated from the light transmittance of the film. The values obtained with the two methods were in excellent agreement.

The structures were milled using a dual beam FIB/scanning electron microscope instrument (FEI Helios NanoLab). The linewidth of the milled structures was controlled by adjusting the ion beam current which resulted in a change in the ion probe diameter. All milling was performed at 30 keV energy of the Ga^+ ions. The parameters of the instrument were optimized by milling a number of test structures close to the edge of the sample. After the optimization was completed the substrate was translated and a set consisting of several copies of the desired structure were milled close to the center of the sample. The structures were separated from each other by at least 150 μm. After optical characterization, one structure from each set was imaged with scanning electron microscope (SEM) to check the quality of the measured structures. In order to avoid carbon contamination of the samples, the structures were in general not imaged with the SEM during the fabrication phase. The optical properties of the structures were found to be essentially identical within a set. Figure 1 shows electron micrographs of the two types of structures studied in this work. Figure 1(a) displays a 25 μm long and 33 nm wide slit. The inset shows a section of the slit at higher magnification. The edge of the slit is straight as seen in the inset. Figure 1(b) shows a cross composed of two 25 μm long and 31 nm wide slits. The other structures studied in this work were of similar high quality without observable defects.

To study the transmission properties of the nanoslits and nanocrosses, the light transmitted through a single structure was imaged onto a spectrometer. The experimental setup is shown in Fig. 2. The sample is placed on an inverted optical microscope and illuminated with polarized light from a tungsten halogen lamp. A long-wave pass colored glass filter is used to suppress higher diffraction orders in the spectroscopic measurements. The light transmitted through the sample is collected with a microscope objective of numerical aperture (NA) 0.75. The NA of the microscope condenser was 0.3 to ensure that the angle of incidence was close to normal. An iris diaphragm placed in the image plane of the microscope was used to select light emerging from a single nanostructure. The distance between the structures was large enough to guarantee that there was no coupling between the neighbouring slits or crosses. The sample was positioned

#110533 - $15.00 USD Received 23 Apr 2009; revised 5 Jun 2009; accepted 7 Jun 2009; published 17 Jun 2009

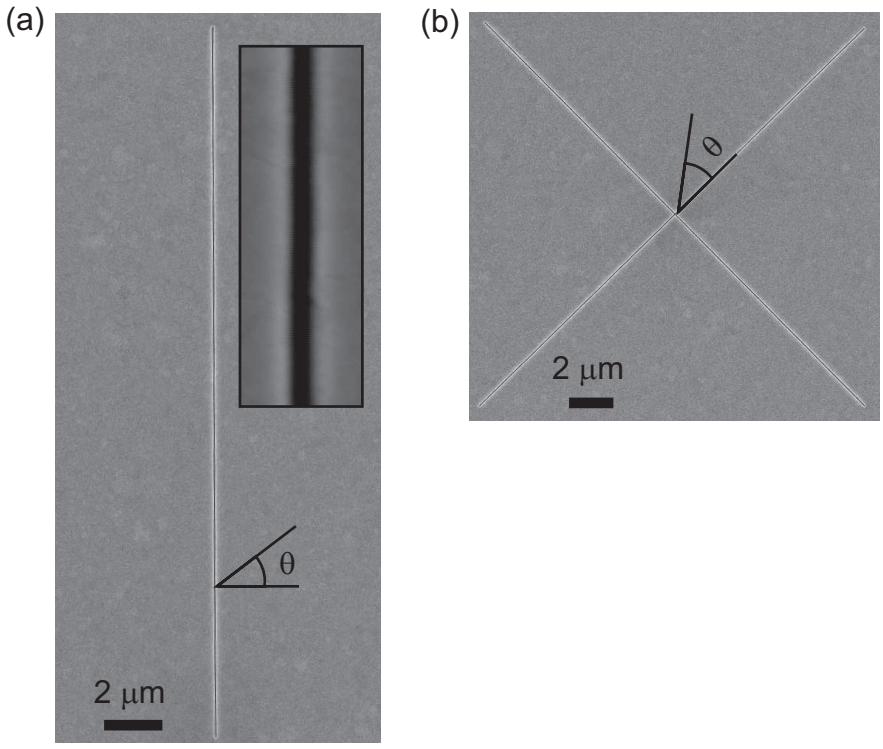

Fig. 1. Scanning electron micrographs of nanoslits fabricated in gold film by focused ion beam milling: (a) 33 nm wide slit and (b) 31 nm linewidth cross. The inset in (a) displays a section of the slit at higher magnification. The angle θ in (a) and (b) defines the direction of polarization of the incident field.

with a piezoelectric stage. The light transmitted through the selected slit or cross could be directed to a charge coupled device (CCD) camera or coupled into a multi-mode optical fiber that guided the light to a grating spectrometer. The spectrometer was equipped with a CCD camera sensitive to the wavelength region 200–1025 nm and an InGaAs linear photodiode array covering the spectral region 0.8–1.7 μm. To compensate for the wavelength dependent transmission of the optical train, the emission spectrum of the lamp, and the wavelength dependent sensitivities of the detectors, a spectrum was collected without the sample. This spectrum was used to normalize the spectra of the light transmitted through the nanostructures. Furthermore, in particular in the visible region of the spectrum, a small amount of light is also transmitted through the gold film. This background was recorded by collecting the transmission spectrum of the sample when no nanostructure was in the field of view and subtracted from the spectra of the light transmitted through the slits or crosses. The spectral transmittance $T(\lambda)$ used in this work is defined as

$$T(\lambda) = \frac{s_{\text{sample}}(\lambda) - s_{\text{film}}(\lambda)}{s_{\text{empty}}(\lambda)}, \tag{1}$$

where $s_{\text{sample}}(\lambda)$ is the signal recorded with the spectrometer at wavelength λ when the light transmitted through the nanostructure was directed to the spectrometer, $s_{\text{film}}(\lambda)$ is the spectrum of the light transmitted directly through the film, and, $s_{\text{empty}}(\lambda)$ is the spectrum recorded without the sample. This definition of the transmittance is the same as the one used in our ear-

#110533 - $15.00 USD Received 23 Apr 2009; revised 5 Jun 2009; accepted 7 Jun 2009; published 17 Jun 2009

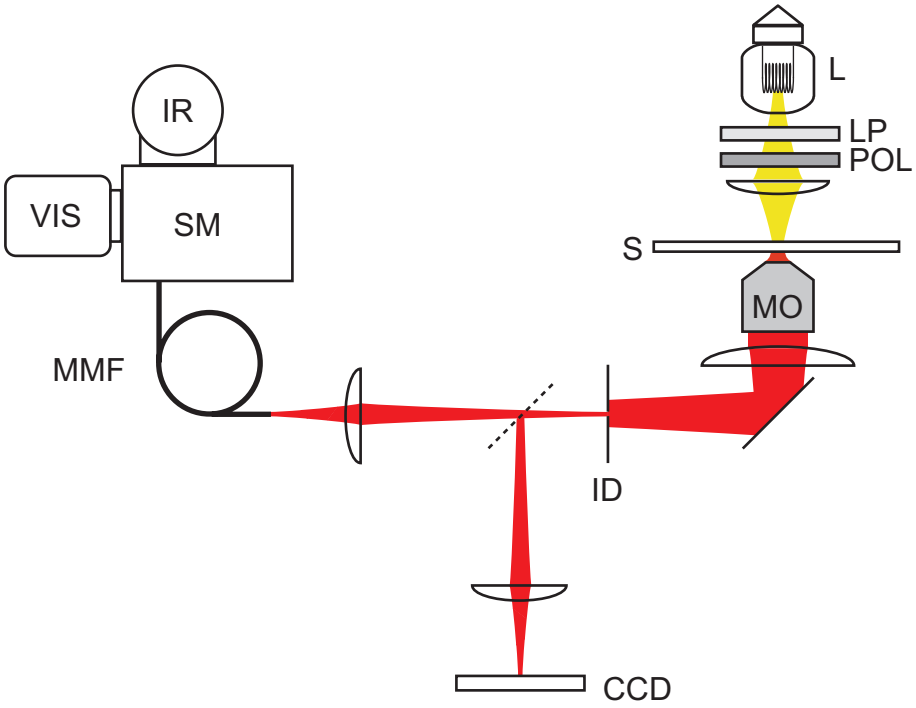

Fig. 2. Experimental setup used to study the nanoslit structures. Light from a tungsten halogen lamp (L) is passed through long-wave pass filter (LP), polarized with a polarizer (POL) and focused on the sample (S). The transmitted light is collected with a microscope objective (MO) and imaged onto either a charge coupled device camera (CCD) or coupled into a multi-mode optical fiber (MMF) that directs the light into a grating spectrometer (SM) equipped with detectors for the visible (VIS) and near-infrared (IR) spectral regions. An iris diaphragm (ID) is used to select only light emerging from one slit.

lier theoretical study of nanoslit transmittance [21]. Differences in integration time and gain of the detectors were taken into consideration by normalizing the collected spectra with the integration time and amplifier gain.

3. Results

Figure 3 shows the slit width dependence of the transmission spectrum of a nanoslit. Also the influence of changing the thickness of the gold film is displayed in Fig. 3. The transmittance values are normalized with the width of the slit to obtain a measure of how much of the light incident on the slit is transmitted through it. We remind here that the slit width was measured not from the slit for which the transmittance is shown in Fig. 3, but, from another slit fabricated in the same milling run with identical parameters as described above. The light transmitted through the slit diverges faster than the light from the lamp when propagating through the setup. This results in a slight decrease of the measured transmittance from its value at the sample plane. In addition, because the reference spectrum recorded without the sample is collected from a much larger area than the slit, the transmittances are given in arbitrary units.

We observe a broad resonance peak in the transmission spectrum of the nanoslits. For the widest slits in the 193 nm thick gold film the resonance is centered at approximately 890 nm

#110533 - $15.00 USD Received 23 Apr 2009; revised 5 Jun 2009; accepted 7 Jun 2009; published 17 Jun 2009

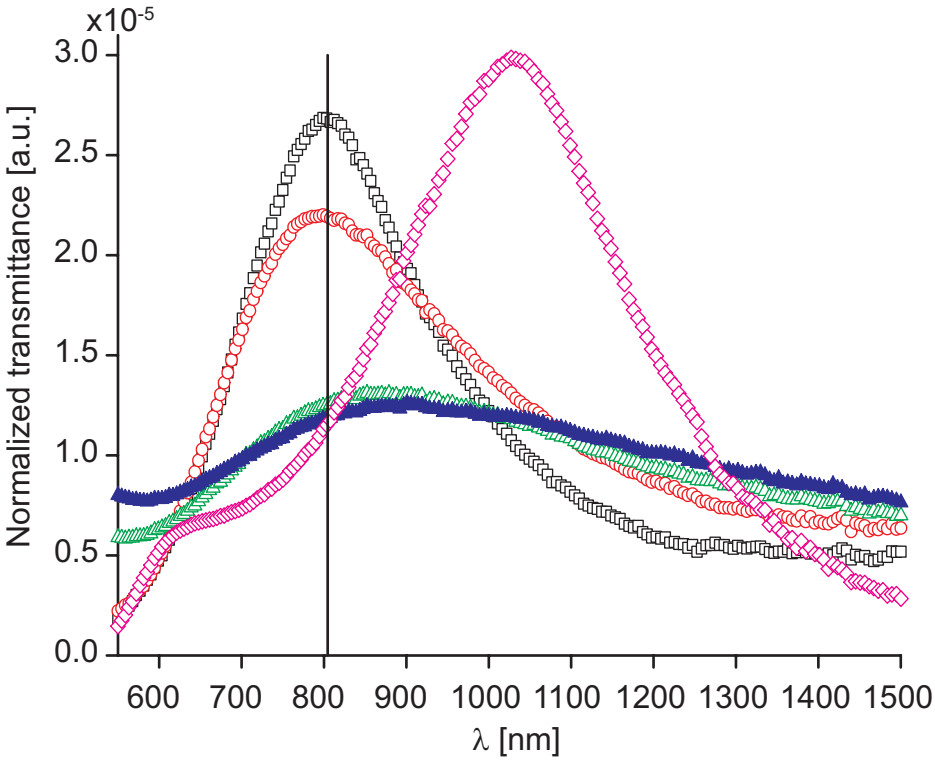

Fig. 3. Normalized transmission spectra of nanoslits of different widths milled in a (193 ± 2) nm thick gold film: 26 nm (black open squares), 35 nm (red open circles), 73 nm (green open triangles), and 85 nm (blue solid triangles) wide slits. The spectrum for a 26 nm wide slit milled in a (270 ± 5) nm thick film is plotted with magenta open diamonds. The spectra have been normalized with the slit width in nanometers. The vertical line indicates the position of the resonance of the most narrow slit of the 193 nm thick film. The polarization of the incident light is orthogonal to the slit ($\theta = 0^\circ$, see Fig. 1).

wavelength while for the narrower slits the transmittance peaks at 800 nm wavelength. The transmission resonance of the slit in the 270 nm thick gold film is centered at longer wavelengths at approximately 1030 nm. In Fig. 3 the polarization of the incident light was set to be perpendicular to the direction of the slits [$\theta = 0^\circ$, see Fig. 1(a)]. For this polarization light can couple to the propagating lowest-order transverse magnetic TM_0 mode in the slit. The Fabry-Pérot (FP) resonances of this propagating light as it is reflected back and forth from the interfaces of the gold film result in the broad peak observed in the transmission spectrum [4, 7, 21].

As the slit becomes narrower the position of the peak first shifts towards shorter wavelengths. Simultaneously, the resonance sharpens. The observed behaviour is in good agreement with our earlier numerical study on the transmission properties of nanoslits [21]. The measured transmission spectra display a similar shape to the numerically calculated ones, Figs. 2 and 6 of [21]. Also the relative heights of the resonance peaks agree well with the theoretical prediction. The position of the resonance peaks in Fig. 3 are slightly blueshifted from numerically calculated resonances for a 200 nm thick gold film [21]. This might be due to the slightly larger film thickness used in those calculations or to differences between the optical properties of the evaporated gold film and the material parameter values used in the theoretical study. The optical properties

#110533 - $15.00 USD Received 23 Apr 2009; revised 5 Jun 2009; accepted 7 Jun 2009; published 17 Jun 2009

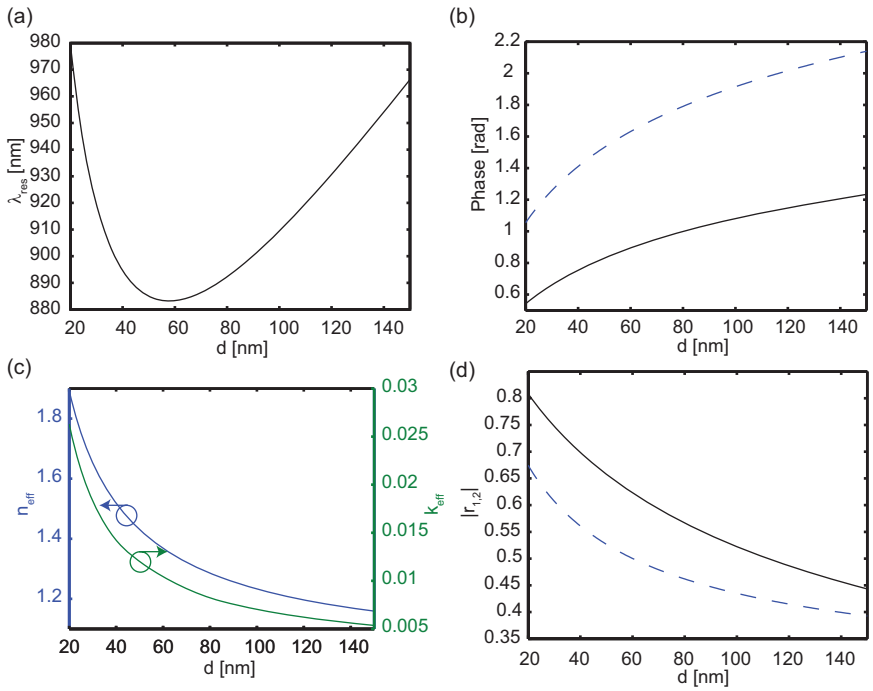

Fig. 4. (a) Theoretically calculated resonance wavelength λ_{res} as a function of waveguide core thickness d. (b) Phase of the reflection coefficient of the waveguide ends with permittivities 1 (black continuous curve) and 2.25 (blue dashed curve) as a function of waveguide core thickness at the corresponding resonance wavelength. (c) The effective index of the mode n_{eff} and the normalized imaginary part of the propagation constant k_{eff} as a function of d at the corresponding resonance wavelength. (d) The dependence on d of the absolute value of the reflection coefficients r_1 and r_2 of the waveguide ends with permittivities 1 (black continuous curve) and 2.25 (blue dashed curve) at the corresponding resonance wavelength. In all calculations the length of the waveguide was $t = 193$ nm and the medium in the waveguide had a permittivity of 1.

of gold are known to depend on sample preparation [22].

The dependence of the position and width of the resonance peak on the slit width can be understood in terms of the properties of the mode that propagates in the subwavelength slit. Treating the slit as a slab waveguide with core thickness d, corresponding to the width of the slit, and length t equal to the thickness of the film, the condition for a Fabry-Pérot resonance becomes [23]

$$2k_0 n_{\mathrm{eff}} t + \phi_1 + \phi_2 = m2\pi, \tag{2}$$

where $k_0 = 2\pi/\lambda_{\mathrm{res}}$ is the free-space wavenumber corresponding to the resonance wavelength λ_{res}, $n_{\mathrm{eff}} = \mathrm{Re}[k_z/k_0]$ is the effective index of the mode with k_z denoting the propagation constant of the mode and Re the real part, ϕ_1 and ϕ_2 are the phase changes at reflection from the ends of the waveguide, and m is an integer. The effective index for a metal-clad waveguide depends strongly on the thickness of the core of the structure and increases as the core becomes thinner [24]. The phase change at reflection from the waveguide end has also been shown to depend on d [23]. In Fig. 4(a) we display the resonance wavelength as a function of waveguide core thickness d, i.e. slit width, obtained by solving numerically Eq. (2) for waveguide

#110533 - $15.00 USD Received 23 Apr 2009; revised 5 Jun 2009; accepted 7 Jun 2009; published 17 Jun 2009

length $t = 193$ nm and $m = 1$. The phases ϕ_1 and ϕ_2 were calculated using the method of [23] and for n_{eff} we used the effective index of the lowest-order even TM mode of a metal-clad waveguide. The values of the phases ϕ_1 and ϕ_2 and the effective index n_{eff} as a function of d at the corresponding resonance wavelength are shown in Figs. 4(b) and 4(c), respectively. Figure 4(c) also displays the value of the normalized imaginary part of the propagation constant $k_{\text{eff}} = \text{Im}[k_z/k_0]$ at the resonance wavelength as a function of d. Here Im denotes the imaginary part. In all calculations we used for the permittivity of gold the values published in [25], interpolating between the data points, and we assumed the waveguide describing the structure to have a core of relative permittivity 1 and to end in regions having permittivities 1 and 2.25.

We observe that as the core becomes thinner the position of the resonance peak first shifts to shorter wavelengths in agreement with the experimental results of Fig. 3. When the thickness is further reduced the peak position starts to shift to longer wavelengths. In the experimental data this is faintly visible. The experimentally observed resonance peaks are at slightly shorter wavelengths than the theoretically calculated values of Fig. 4(a). As noted above, this might be due to differences between the optical properties of the evaporated gold film and the material parameter values used in the calculations. We note that the resonance wavelengths obtained by solving Eq. (2) agree rather well with the results of [21] which were obtained by rigorously solving Maxwell's equations for the slit structure. Figure 4(d) displays the absolute value of the reflection coefficients r_1 and r_2 of the ends of the waveguide. As expected, the magnitude of the reflection coefficient increases as the core becomes thinner resulting in a higher quality factor of the resonance in agreement with the experimental data.

When the gold film becomes thicker, the position of the transmission resonance is observed to shift significantly to the red (see Fig. 3). The shape and width of the peak is not seen to change significantly except for becoming slightly more symmetric. The asymmetry of the resonance peak for the 193 nm thick metal film is most likely due to the high losses of the propagating mode for visible wavelengths so that the short wavelength side of the peak is more strongly attenuated than the long wavelength side. The shift in the peak position as the film thickness is increased can also be related to the propagating mode. Viewing the slit as a resonator, a thicker gold layer corresponds to increasing the length of the cavity which leads to a shift of the resonance. Comparing the resonance wavelengths for the two 26 nm wide slits we see that Eq. (2) is approximately satisfied even assuming n_{eff}, ϕ_1 and ϕ_2 to be independent of wavelength. In the numerically simulated spectra of [21] we observed a shift of 200 nm in the position of the resonance peak of a 40 nm wide slit when the film thickness was changed from 200 nm to 275 nm. Solving Eq. (2) numerically as described above, we obtain a shift of 270 nm for the position of the resonance peak. These values are in relatively good agreement with the experimentally observed shift of approximately 230 nm.

Ideally, a slit is a two-dimensional structure that should be infinitely long. To study the influence of the length of the slit on the transmission spectrum we fabricated a set of 33 nm wide slits the length of which was varied between 25 μm and 1.25 μm. The transmittances of these slits are shown in Fig. 5. As can be seen, the shape of the spectrum is hardly modified, even when the slit is made significantly shorter. We remark here that the spectra have been normalized with the slit length in order to better illustrate the spectral features. For the shortest slit, we can see some changes in the spectrum as the length of the structure approaches the wavelength. At this point the slit resembles more a rectangle than a slit and consequently the spectrum starts to become attenuated by more than the geometrical shortening of the length of the slit would suggest. It is interesting to note that Matteo *et al.* observed in their study of nanoapertures that a rectangular aperture transmitted considerably more light than a square one of the same area [26]. Although the length of the rectangles used in that study were somewhat smaller than the length of the shortest slit studied here, our results indicate that this observation might partly

#110533 - $15.00 USD Received 23 Apr 2009; revised 5 Jun 2009; accepted 7 Jun 2009; published 17 Jun 2009

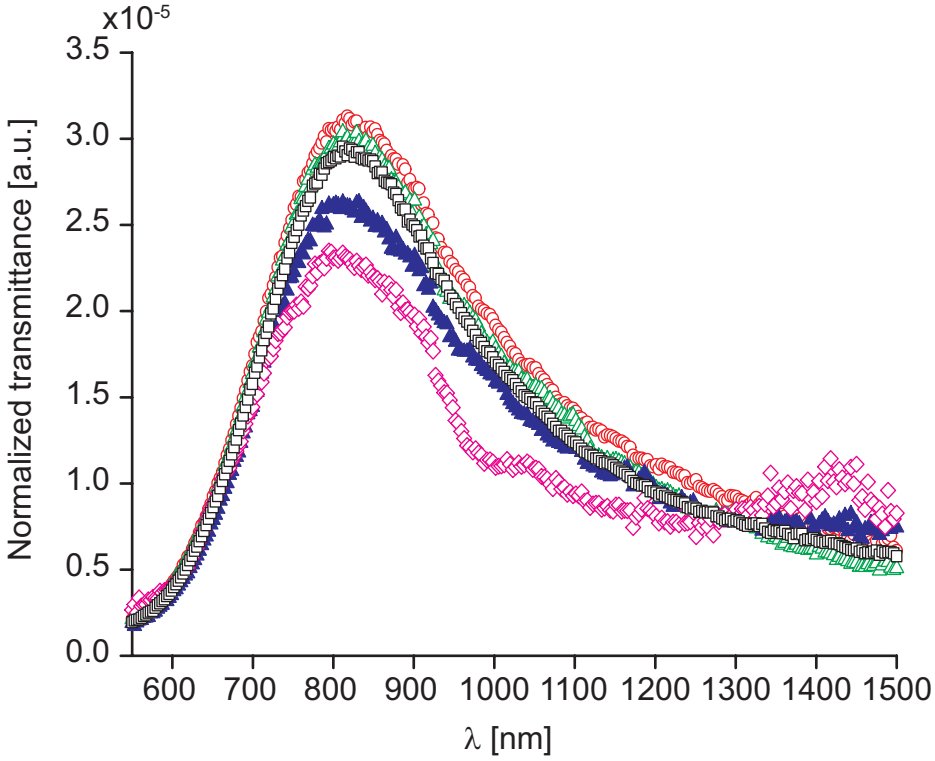

Fig. 5. Transmission spectra of 33 nm wide slits in 193 nm thick gold film for different slit lengths: 25 μm (black open squares), 10 μm (red open circles), 5 μm (green open triangles), 2.5 μm (blue solid triangles), and 1.25 μm (magenta diamonds). The spectra were normalized with the slit length in micrometers. The polarization of the incident light is orthogonal to the slit ($\theta = 0^\circ$, see Fig. 1).

be due to waveguiding.

So far the polarization direction of the incident light has been fixed to be orthogonal to the slit so that the light can couple to the mode propagating in the slit. If the polarization is rotated, the transmittance of the slit is strongly attenuated. Figure 6(a) displays the transmission spectrum of a 33 nm wide and 25 μm long slit as a function of the polarization direction. The spectrum for the polarization direction $\theta = 4^\circ$ is shown in Fig. 6(b). If two nanoslits are milled orthogonal to each other in the form of a cross as shown in Fig. 1(b), this polarization dependence disappears. The measured transmission spectrum of such a cross composed of two 31 nm wide slits as a function of the incident polarization direction is shown in Fig. 6(c). The spectrum remains essentially unchanged as the polarization direction is rotated a full circle. In these measurements only one of the detectors on the spectrometer was used in order to prevent the measurements from becoming excessively long. As a consequence, the spectral range of the data is 550–1000 nm. Surprisingly, the shape of the spectrum is almost exactly the same as that of the simple slit as seen when comparing Figs. 6(b) and 6(d) which display the transmittance spectra of the slit and cross for the direction $\theta = 4^\circ$, respectively. It seems that the intersection region in the cross structure does not significantly affect the optical properties of the two slits.

The difference in the transmission properties of the slit and cross are seen clearly when

#110533 - $15.00 USD Received 23 Apr 2009; revised 5 Jun 2009; accepted 7 Jun 2009; published 17 Jun 2009

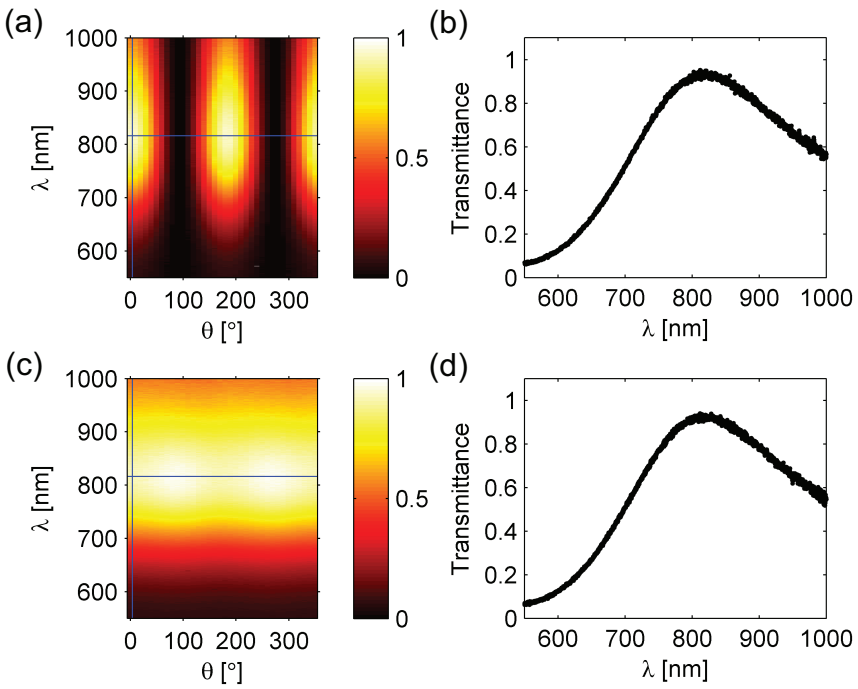

Fig. 6. Transmission spectra of ≈ 30 nm wide slit and cross structures in 193 nm thick gold film as a function of the polarization direction θ (see Fig. 1) of the incident field: (a) spectral transmittance of a 25 μm long and 33 nm wide slit as a function of θ, (b) transmission spectrum of the slit for $\theta = 4^\circ$, (c) spectral transmittance of a cross composed of two 25 μm long and 31 nm wide slits as a function of θ, and (d) transmission spectrum of the cross for $\theta = 4^\circ$. The spectra have been normalized by the maximum transmittance of the cross. In (a) and (c) the vertical line is along the cross section $\theta = 4^\circ$.

comparing the polarization dependence of the peak transmittances for the two structures shown in the polar plot of Fig. 7. It can be seen that the slit transmits hardly any light when the polarization of the incident light is along the direction of the slit. As a matter of fact, the slit operates as a polarizer transmitting only the component of the electric field in the direction orthogonal to the slit. This is seen from the fit of a $\cos^2\theta$ curve in Fig. 7. The maximum transmittance of the cross, on the other hand, is much less dependent on the polarization. Only a small variation can be seen in the peak transmittance as the polarization is rotated. This is probably due to a small difference in the widths of the two slits making up the cross. The fact that the slit functions as a polarizer is in agreement with the simple model that the transmission mechanism is by coupling to the propagating mode of the slit.

We have seen that the transmission spectrum of the nanoslit is highly sensitive to the width of the slit and the thickness of the gold film whereas changing the length of the structure does not significantly alter the transmittance. For applications in sensing and switching, a central question is the dependence of the transmission spectrum on the presence of a disturbance in the slit. To investigate this, we applied a drop of 1,9-nonanedithiol to the structure. This substance has a refractive index of 1.494 ($\lambda = 589$ nm) [27] and readily penetrates into the slit to act as a disturbance. The transmittance spectrum of a 26 nm wide slit milled in a 270 nm thick

#110533 - $15.00 USD Received 23 Apr 2009; revised 5 Jun 2009; accepted 7 Jun 2009; published 17 Jun 2009

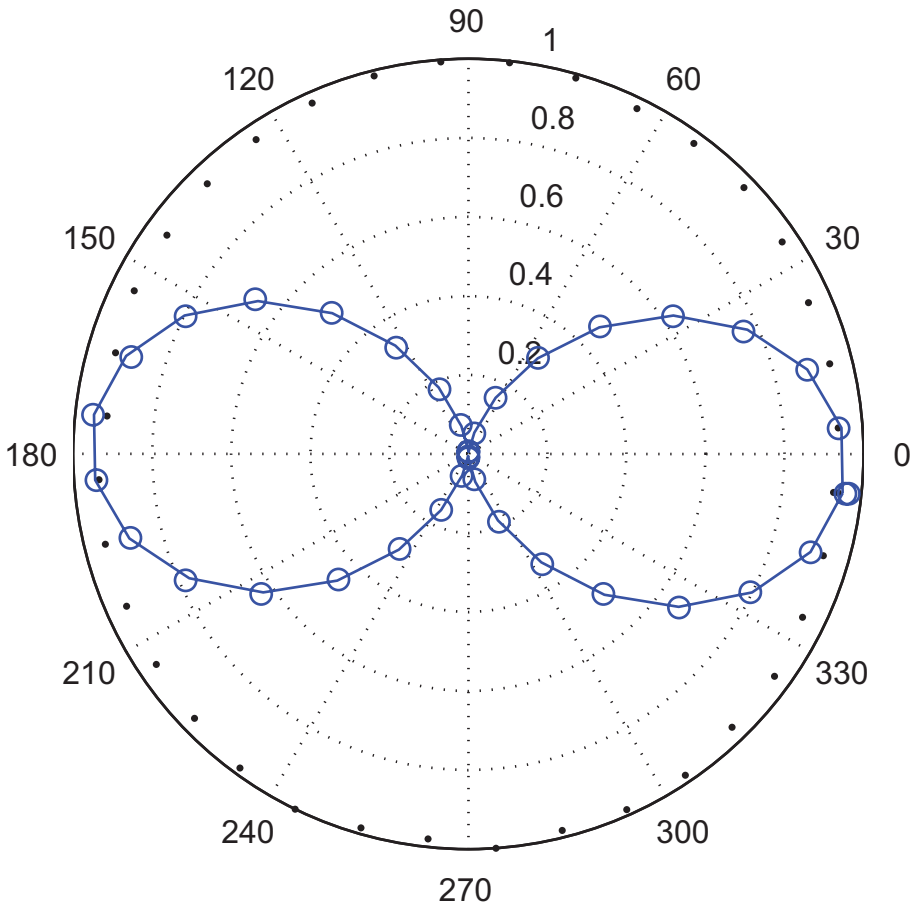

Fig. 7. Polar plot of the maximum transmittance of the cross and slit structures as a function of the polarization direction θ of the incident field. The figure shows the transmittance along the horizontal line in Figs. 6(a) and 6(c) for the cross (black points) and the slit (blue circles), respectively. The solid line is a $\cos^2\theta$ fit to the data for the slit. The data point for $\theta = -6^\circ$ was the start point and was measured a second time after completing a full circle. The data was normalized with the peak transmittance of the cross.

#110533 - $15.00 USD Received 23 Apr 2009; revised 5 Jun 2009; accepted 7 Jun 2009; published 17 Jun 2009

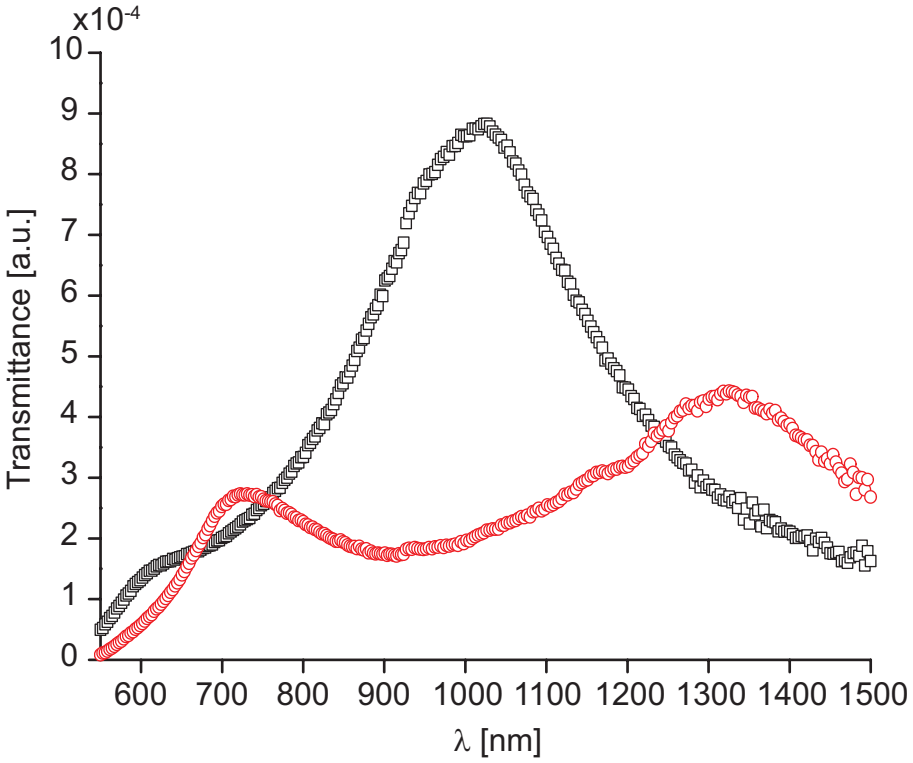

Fig. 8. Change in transmission spectrum when a drop of 1,9-nonanedithiol is applied to the sample: transmission spectrum of a 26 nm wide slit milled in a 270 nm thick gold film for air (black open squares) and 1,9-nonanedithiol (red open circles) in the slit.

gold film was measured before applying the liquid and again with the liquid in the slit. The spectra are shown in Fig. 8. We observe a large shift of approximately 300 nm in the position of the transmission peak. At the same time, the next FP resonance peak appears from the short wavelength side of the spectrum. The large shift in the spectrum demonstrates that this type of structure is well suited for sensing changes in the refractive index or to control light by altering the refractive index of the medium within the slit. The two FP resonances visible in the spectrum with 1,9-nonanedithiol in the slit can also be used to estimate the effective index of the propagating mode using Eq. (2) if we neglect the wavelength dependence of n_{eff}, ϕ_1, and ϕ_2. The value obtained in this way is 3.0. Theoretically we obtain 2.8 for $\lambda = 726$ nm and 2.5 for $\lambda = 1324$ nm. The simple estimate from the measured data is in a rather good agreement with these values. In numerically calculated spectra the resonance peak for a 15 nm wide slit was observed to shift by 8 nm for a refractive index change of 0.01 [21]. The shift of approximately 6 nm for the same change in the refractive index observed here for the wider slit (26 nm) is in good agreement.

4. Conclusions

We have experimentally studied light transmission through isolated narrow, nanometer-scale slits and crosses in a gold film. Our results are in good agreement with our earlier numerical study of the light transmission properties of nanoslits [21]. The observed behaviour of the trans-

#110533 - $15.00 USD Received 23 Apr 2009; revised 5 Jun 2009; accepted 7 Jun 2009; published 17 Jun 2009

mission spectrum as the parameters of the structure are varied can be explained by viewing the slit as a low Q-factor resonator. The resonance can be used both to sense changes in the medium within the slit as well as to control the transmitted light spectrum by tuning the refractive index of the material in the slit. Our results also show that such a structure can be made short without altering the optical properties. The transmission spectrum starts to change only when the length of the slit approaches the wavelength of the light. Using the dimensions of the structures studied in this work, volumes of 10^{-17} liter could be used in such applications.

The cross structure offers many interesting possibilities in realizing photonic nanostructures. As demonstrated in this work, the transmission spectrum of the cross is independent of the polarization, a useful property in many cases. The fact that the transmission properties of the two slits are not affected by the intersection region opens up possibilities in creating structures where light of different polarization is spatially resolved. By using crosses with smaller dimensions it would also seem to be possible to create arrays of such structures that would combine the high transmittance of the individual element as well as the possibility of launching surface waves along the periodically patterned surface.

Acknowledgements

This research was financially supported by the Academy of Finland (project number 118074). K. Lindfors and L. Lechner acknowledge grants from the Vilho, Yrjö and Kalle Väisälä fund and the Emil Aaltonen foundation, respectively.

#110533 - $15.00 USD Received 23 Apr 2009; revised 5 Jun 2009; accepted 7 Jun 2009; published 17 Jun 2009